A THESIS FOR THE DEGREE OF
MASTER OF SCIENCE IN FOOD AND NUTRITION

Roles of Taste 1 Receptor 3 in Development of Diet-induced Obesity

식이 유도 비만 발생과정에서의

Taste 1 Receptor 3의 역할 연구

August, 2021

Department of Food and Nutrition
Graduate School
Seoul National University
Seung Hoon Oh

Roles of Taste 1 Receptor 3 in Development of Diet-induced Obesity

식이 유도 비만 발생과정에서의 Taste 1 Receptor 3의 역할 연구

지도교수 신 동 미

이 논문을 생활과학 석사학위 논문으로 제출함

2021 년 7 월

서울대학교 대학원

식품영양학과

오 승 훈

오 승 훈의 생활과학 석사학위 논문을 인준함

2021 년 7 월

위 원 장 _____

부위원장 _____

위 원 _____

Abstract

Roles of Taste 1 Receptor 3 in Development of Diet-induced Obesity

Seung Hoon Oh

Department of Food and Nutrition

The Graduate School

Seoul National University

Worldwide spread of obesity and its increasing prevalence have been the root of various metabolic diseases such as coronary heart disease, diabetes, and non-alcoholic fatty liver disease and investigation on its cause and prevention is important to public health. Western diet, characterized by high fat diet and sugar sweetened beverage, is one of the major environmental factors on obesity development. However, the molecular mechanism of how western diet induces obesity is yet to be fully discovered. Recently, taste receptors, thought only to be expressed in the tongue, are reported to be expressed in extra-oral tissues. However, the role of taste receptors in extra-oral tissues, other than taste sensing, is not well studied. Taste 1 receptor 3 (TAS1R3) is

known for sensing sweet and umami taste in the tongue, but the role in other tissues in obesity development is not discovered. In this research, the role of taste receptor TAS1R3 in obesity development was studied. In order to investigate the role of TAS1R3, knockout mice were used to compare physiological and molecular changes in development of obesity to normal wildtype mice. 8-12 weeks old *Tas1r3*$^{-/-}$ (KO) and *Tas1r3*$^{+/+}$(WT) mice were fed normal diet (ND) or western diet (WD; 60% fat diet + 30% sucrose water) for 14 weeks (n=20-30/group). During 14 weeks of diet induction, normal diet fed WT and KO mice had no body weight difference. As expected, the WD fed WT mice had dramatic body weight gain. However, WD fed KO mice had significantly low body weight gain compared to WT mice. Body composition analysis revealed that WT mice had high fat percentage (36.8%) while KO mice did not (22.7%). Metabolic analysis showed that KO-WD mice had unaffected respiratory exchange ratio in contrast to WT-WD. Interestingly, WT and KO mice groups did not have different food intake and activity rate. To investigate the underlying cause of different obesity development in WT and KO mice, transcriptome analysis of intestinal tissues was carried out. PCA and hierarchical clustering analysis showed that WD fed WT and KO mice had significantly different transcriptome. Analysis on differentially expressed genes showed that the genes related to lipid absorption and metabolism (CD36, mTOR, SREBP) are down regulated in KO-WD mice. GLP-2

receptor expression in enterocyte were also down regulated in KO-WD mice (2.1 RPKM vs. 3.6 RPKM). Gene interaction network analysis revealed that KO mice had reduced gene networks related to lipid absorption and metabolism (mTOR and SREBP). Investigation into the actual lipid absorption in the intestines of WD fed WT and KO mice were different. KO-WD mice excreted more lipids in feces. Analysis with fat intake showed that WT-WD mice excreted steady level of lipids. However, KO-WD mice excreted more lipids with more fat intake ($p=0.0364$). Also, the intestinal lipid level after olive oil gavage showed that KO-WD mice had more unabsorbed residual lipids in the intestinal tissue. In conclusion, this study proposes new roles and molecular mechanism of TAS1R3 in development of western diet induced obesity.

Keywords **:** TAS1R3 (Taste 1 receptor member 3), Obesity, Western diet, Lipid absorption

Student Number **:** 2019-21991

Contents

List of Tables

List of Figures

List of Abbreviations

ANOVA	Analysis of variances
BMI	Body-mass index
cAMP	Cyclic adenosine monophosphate
CD36	Cluster of differentiation 36
CHD	Coronary heart disease
CLAMS	Comprehensive lab animal monitoring system
DEG	Differentially expressed gene
DM2	Type 2 diabetes mellitus
EEC	Enteroendocrine cell
FDR	False discovery rate
GLP	Glucagon-like peptide
GLUT2	Glucose transporter 2
H&E	Hematoxylin and eosin
HCL	Hierarchical clustering

IPA	Ingenuity pathway analysis
KO	Knockout
MTORC1	Mammalian target of rapamycin complex 1
ND	Normal diet
PCA	Principal component analysis
PEPT1	Peptide transporter 1
PPAR	Peroxisome proliferator-activated receptor
ROS	Reactive oxygen species
RPKM	Reads per kilobase of transcript, per million mapped reads
SEM	Standard error of mean
SREBP	Sterol regulatory element-binding protein
SGLT1	Sodium-dependent glucose transporter isoform 1
TAS1R3	Taste 1 receptor 3
TC	Total cholesterol
TG	Triglyceride

TP	Total protein
WD	Western diet
WAT	White adipose tissue
WT	Wild type

I. Introduction

1. Obesity

Obesity is defined by body-mass index of over 30kg/m^2 (Kopelman, 2000). People with obesity is often associated with type 2 diabetes mellitus (DM2), coronary heart disease (CHD), certain types of cancers, and depression (Bhaskaran, et al., 2014; Luppino et al., 2010). The mortality rate of normal weight individuals who had been obese was about 3 times higher than individuals who had never exceeded normal weight (Xu et al., 2018). Due to its association with other health complications and mortality, obesity has become a major public health issue and economic burden in many societies (Cameron et al., 2004; Tremmel et al., 2017). While the dangers of obesity have caught the attention, centers for disease control and prevention (CDC) has reported that the obesity prevalence has increased to 42.4% from 30.5% during 1999 and 2018 in overall US population (Hales, et al., 2020). Korea centers for disease control and prevention (KCDC) also reported that the prevalence of obesity was 34.8% in 2016. Despite the attention and effort to prevent and treat obesity, the major public health issue is on the rise.

2. Western diet

Factors that influence obesity could be divided into two groups: environmental factors and genetic factors (Conway & Rene, 2004). Environmental factors include, food intake, exercise, and culture (Kopelman, 2000). Excessive food intake has been one of the leading causes of obesity. Especially, western diet, characterized by its high composition of fat and carbohydrate, is associated to obesity development (Hu et al., 2001). Western diet is known to increase reactive oxygen species (ROSs) and inflammation which leads to insulin resistance and other metabolic imbalances in the body (Kopp, 2019). Various reports have revealed that western diet affects lipid metabolism and oxidative stress in liver tissues (Renaud et al., 2014; Lee, 2015; Park, 2017). Through some molecular mechanisms, inhibiting nutrient absorption, reducing hunger or appetite, inhibiting nutrient metabolism in mitochondria and such were used for treating obesity but each had severe side effects (Filippatos et al., 2008; Khera et al., 2016). While various mechanisms and treatments have been introduced to prevent and treat obesity, the increasing obesity prevalence implies that new approach to obesity and diet is required (Jackson et al., 2015).

3. Taste receptors

Taste receptors, originally thought to be only expressed in the tongue and sense tastes, are highly expressed in extra-oral tissues such as intestine, testis, or lung (Depoortere, 2014; Mosinger et al., 2013; Merigo et al., 2012). Taste 1 receptor 3 (TAS1R3) is especially highly expressed in the small intestine. In the tongue, TAS1R3 recognizes sugar and amino acids and senses sweet and umami taste by forming heterodimers with TAS1R2 and TAS1R1, respectively. The TAS1R3 deficient mice are reported to have impaired glucose metabolism with low insulin sensitivity and glucose tolerance (Murovet et al., 2014; Murovet et al., 2015.; Murovet et al., 2019,). The knockout mice also have reduced atherosclerotic plaque accumulation but all the mechanisms are not well studied (Shojaat et al., 2020). Also, in pancreatic beta cells, which secretes insulin to the blood the blood stream, TAS1R3 is expressed. TAS1R3 is reported to regulate signals of alpha-gustducin and cyclic adenosine phosphate (cAMP) signaling pathway (Udagawa et al., 2020). In the intestine, TAS1R3 is known to regulate the expression of sodium-glucose transporter 1 (SGLT1) in enterocytes and glucagon-like peptide 1 (GLP1) hormone secretion in enteroendocrine cells (Margolskee et al., 2007; Wang et al., 2018). However, the exact mechanisms of how TAS1R3 regulates SGLT1 expression or GLP1 secretion are not discovered. Another research has shown that TAS1R3 deficient mice are resistant to diet-induced

gut inflammation through regulation of gut microbiota and observed little increase in body weight (Shon, 2021). While TAS1R3 is expected to play a role in nutrient absorption or incretin mediated metabolism and other nutrient related functions in the intestine, no study has touched on the subject. Moreover, the role of intestinal TAS1R3 in development of obesity induced by western diet is yet to be uncovered.

4. Aim of this study

The objectives of this study were, (i) to determine whether TAS1R3 plays a role in development of obesity induced by western diet, (ii) to understand the transcriptional networks regulated by intestinal TAS1R3, and (iii) to demonstrate the effects of absence of intestinal TAS1R3 on obesity development.

II. Materials and Methods

1. Animals

Tas1r3$^{-/-}$ mice with C57BL/6J genetic background were purchased from Jackson Laboratory (Bar Harbor, ME, USA). Tas1r3$^{-/-}$ mice were crossed with C57BL/6J wild-type to generate *Tas1r3*$^{+/+}$ and *Tas1r3*$^{-/-}$ littermates used in this study. Genotypes were identified by PCR after 4 weeks from birth. All mice were fed standard chow diet (Purina Korea Inc., Seoul, Korea) and plain water *ad libitum* until the experiments. Male and female littermates were housed in specific pathogen free (SPF) facility at the Seoul National University College of Veterinary Medicine (Seoul, Korea). All experimental procedures were approved by the Committee on the Ethics of animal experiments of Seoul National University (Institutional Animal Care and Use Committee permit number: SNU-181001-2).

2. Diet-induced Obesity Model

8-12 weeks old male and female mice were subjected to diet induced obesity model. 3-4 littermates were housed in each cage. Western diet group received high fat diet with 60 kcal% fat (D12492, Research Diets Inc, New Brunswick NJ, USA) and 30% (w/v) sucrose solution. Control group received normal diet

with 10 kcal% fat (D12450J) and plain water. All foods and drinks were supplied *ad libitum* for 14 weeks. A summary of experimental groups is provided in **Table 1.** and nutritional information of diet used in the experiments is presented in **Table 2**. Body weight, food and drink intake were monitored two times a week.

Table 1. Experimental Groups

Groups	Diet scheme	Body weight change (n)	Metabolic cage (n)	Histology (n)	RNA-sequencing (n)	Fecal lipid (n)	Olive oil gavage (n)
WT ND	Normal diet[1)] + Tap water	20	7	4	-	-	-
KO ND	Normal diet + Tap water	20	5	4	-	-	-
WT WD	High fat diet[2)] + Sugar drink[3)]	30	11	4	6	9	5
KO WD	High fat diet + Sugar drink	30	11	4	6	9	5

[1)] 10Kcal% fat (D12450J, Research Diets Inc., New Brunswick, NJ, USA)

[2)] 60Kcal% fat (D124592, Research Diets Inc., New Brunswick, NJ, USA)

[3)] 30% (w/v) sucrose solution

Table 2. Composition of experimental diets

	D12450J (Normal-fat diet)		D12492 (High-fat diet)	
	g%	**kcal%**	**g%**	**kcal%**
Fat	4.3	10	35	60
Carbohydrate	67.3	70	26	20
Protein	19.2	20	26	20
Total (%)	100		100	
kcal/g	3.85		5.24	

Ingredients	**g**	**kcal**	**g**	**kcal**
Casein, 30 Mesh	**200**	**800**	**200**	**800**
L-Cysteine	**3**	**12**	**3**	**12**
Corn Starch	**506.2**	**2024.8**	**0**	**0**
Maltodextrin 10	**125**	**500**	**125**	**500**
Sucrose	**68.8**	**275.2**	**68.8**	**275**
Cellulose, BW 200	**50**	**0**	**50**	**0**
Soybean Oil	**25**	**225**	**25**	**225**
Lard	**245**	**180**	**245**	**2205**
Mineral Mix S10026	**10**	**0**	**10**	**0**
DiCalcium Phosphate	**13**	**0**	**13**	**0**
Calcium Carbonate	**5.5**	**0**	**5.5**	**0**
Potassium Citrate, 1 H_2O	**16.5**	**0**	**16.5**	**0**
Vitamin Mix V10001	**10**	**40**	**10**	**40**
Choline Bitartrate	**2**	**0**	**2**	**0**
FD&C Blue Dye #1	**0.01**	**0**	**0.05**	**0**
FD&C Yellow Dye #5	**0.04**	**0**	**0**	**0**
Total	**1055.05**	**4057**	**773.85**	**4057**

(information provided by Research Diets Inc., New Brunswick, NJ, USA)

3. Metabolic Studies

After 14 weeks of diet induction, 5-11 mice were randomly selected from each group and were put in CLAMS metabolic cages. For 2 days mice were acclimated to the cages and for another 2 days body composition, energy expenditure, RER, and activity were measured. During the 4 days in the metabolic cages, mice had *ad libitum* access to food and water according to each diet group.

4. Sample Collection

All mice were fasted overnight (12 hours) before sacrifice. After fasting, mice were anesthetized by intraperitoneal injection of 20% (w/v) urethane solution (1.0-1.5 mg/g body weight). Whole blood samples were collected by carotid artery incision and centrifuged at 2,000 rpm for 20 minutes. Serum samples were carefully separated from the supernatant. The liver, abdominal fat, and small intestine were excised and snap frozen in liquid nitrogen. All collected samples were stored at -80°C until further experiments.

5. Fecal Lipid Analysis

After 14 weeks of diet induction, randomly selected 6-9 mice from each group were put in single housing. After 48 hours in single housing, feces were collected. Body weight, diet and water intake were measured. Collected feces were weighted and freeze dried for 24 hours. Fecal lipid was extracted with slightly modified Folch's method (Folch, Lees & Sloane-Stanely, 1957). 100 mg of feces were weighed and placed in 2.0 ml round bottomed polypropylene tubes with 500 ul 0.9% (w/v) NaCl solution. The samples were homogenized with TissueLyser II (Qiagen, Hilden, Germany) and 5 mm stainless steel beads (Qiagen, Valencia, CA, USA) at 30 Hz for 30 seconds. After homogenization, 500 ul of chloroform:methanol (2:1) were added and vortexed thoroughly. Mixtures were centrifuged at 1,000 x g for 10 minutes. The under-phase chloroform containing lipids were carefully separated into new polypropylene tubes, died under a fume hood, and weighed for remaining lipids.

6. Olive Oil Gavage

After feces collection, nine western diet fed mice were randomly selected from each genotype. After overnight (12 hours) fasting, olive oil (1.0 mg/g

body weight) gavage was performed to each mouse. After 4 hours from gavage, mice were anesthetized and intestinal tissues were collected as mentioned above.

7. Histological Analysis

During sample collection, small parts of adipose tissues, liver tissues, and small intestine tissues were excised separately for histological analyses. They were fixed with 10% formaldehyde overnight, and stored at 4°C until further experiments. Fixed tissues were incised for 2-3mm thickness, suitable size for tissue preparation. For hematoxylin and eosin (H&E) staining, the incised tissues were processed (STP120 Spin tissue processor, Thermo Fisher Scientific, Rockford, IL, USA) for 13 hours. Microtome (Shandon Finesse ME Microtome, Thermo Fisher Scientific, Rockford, IL, USA) was used to cut the samples for 3um thickness, and the sections were attached to the slides for washing and stained. All slides were scanned with Motic Easyscan One (Myer Instruments, Houston, TX, USA). ImageJ software (NIH, Bethesda, MD, USA) was used to quantify and measure the size of adipocytes and liver fat droplet area (Parlee et al.,2014).

8. Intestinal TG Analysis

Small intestine samples stored at -80°C, were thawed and weighed. Samples were homogenized and total lipids were extracted by slightly modified Folch's method (Folch, Lees & Sloane-Stanely, 1957). The chloroform was dried with HyperVAC-Max (Labogene, Seoul, Korea) at 2000g, 4°C for 2 hours. The dried lipid pellets were suspended in 120 ul of isopropanol. The intestinal TG and TC concentration was measured by commercial kit mentioned above (Asan Pharmaceutical Company, Seoul, Korea). The intestinal proteins were extracted with the use of T-PER tissue protein extraction reagent (Thermo Scientific, Rockford, IL, USA) as the diluent. The protein levels were measured with Micro BCA protein assay kit (Thermo Scientific, Rockford, IL, USA) as described in the enclosed protocol.

9. RNA-sequencing

Total RNA from small intestine was isolated with DNA-free RNA isolation kit (Ambion, Austin, TX, USA), according to manufacturer protocol. Total RNA quality and quantity were assessed with NanoDrop 2000 spectrophotometer (Thermo Fisher Scientific, Waltham, MA, USA). Isolated RNA samples were amplified by RNA amplification kit (Ambion, Austin, TX, USA) according to the provided protocol. cRNA quality and quantity were assessed

with NanoDrop 2000 spectrophotometer (Thermo Fisher Scientific, Waltham, MA, USA). cRNA hybridization on MouseWG-6 Expression BeadChip arrays (Illumina Inc., San Diego, CA, USA) was carried out according to the provided protocol. The arrays were scanned with the BeadStation 500G Instrument (Illumina Inc., San Diego, CA, USA), and Spot image identification and quantification were processed by Genome Studio software v1.0.2. (Illumina Inc., San Diego, CA, USA).

10. Statistical Analysis

All data were presented as mean ± SEM. Statistical significance (p value < 0.05) was evaluated by unpaired student's t-test between two groups or one-way analysis of variance (ANOVA) of multiple groups followed by Tukey's test for post hoc analysis. Analysis of covariance was performed to analyze the effect of covariates (Tschöp et al., 2011). Graph Pad Prism 9 software (GraphPad Software Inc., La Jolla, CA, USA) were used for statistical analyses. For gene analyses Ingenuity pathway analysis (IPA) (Qiagen, Redwood City, CA, USA) was used.

III. Results

1. Tas1r3 knockout mice are resistant against diet-induced obesity

To identify the role of Tas1r3 in diet induced obesity, adult *Tas1r3*$^{+/+}$ and *Tas1r3*$^{-/-}$ mice were challenged with ND or WD for 14 weeks. When treated with ND, *Tas1r3*$^{+/+}$ mice and *Tas1r3*$^{-/-}$ mice showed no difference in body weight gain. However, after stimulation with WD, *Tas1r3*$^{+/+}$ mice, compared to *Tas1r3*$^{-/-}$ mice, showed great increase in body weight ($P<0.001$). While the average male final body weight for WD fed *Tas1r3*$^{+/+}$ group was 42.16g, *Tas1r3*$^{-/-}$ group was 30.82g ($P<0.001$). In case of female mice, 37.32g vs. 26.56g was observed ($P<0.005$). The tendency between genotypes were same in both sex groups and in further analyses male and female groups were combined (**Figure 1**).

The results from CLAMS analysis indicate the little body weight gain majorly comes from different degree in fat composition. While *Tas1r3*$^{+/+}$ mice had 36.8% fat, *Tas1r3*$^{-/-}$ mice had 22.7% fat ($P<0.005$). ANCOVA of energy expenditure with lean body mass showed WD treated *Tas1r3*$^{+/+}$ mice have low energy expenditure compared to *Tas1r3*$^{-/-}$ mice ($P<0.005$) while lean body mass has no effect on energy expenditure. In addition, only WD fed

Tas1r3$^{+/+}$ mice had decreased RER level ($P<0.05$), signifying a preference for fat as the main metabolic substrate (**Figure 2**).

Histological analysis of white adipose tissues from four experimental groups revealed that, in accordance with body composition analysis, only western diet fed *Tas1r3*$^{+/+}$ mice had enlarge adipocytes ($P<0.0001$). *Tas1r3*$^{-/-}$ mice showed no increase in size of adipocytes ($P=0.5492$). **(Figure 3**). Histological analysis of liver tissues also showed similar outcome. Only western diet fed *Tas1r3*$^{+/+}$ mice had developed lipid droplets in the liver ($P<0.0004$). Contrastingly, *Tas1r3*$^{-/-}$ mice did not develop fatty liver with western diet ($P=0.8333$) **(Figure 4).**

Collectively, under normal environment, there were no disparity between two genotypes, but under metabolic stress, *Tas1r3*$^{-/-}$ mice had little or no obesity related disruptions, unlike *Tas1r3*$^{+/+}$ mice.

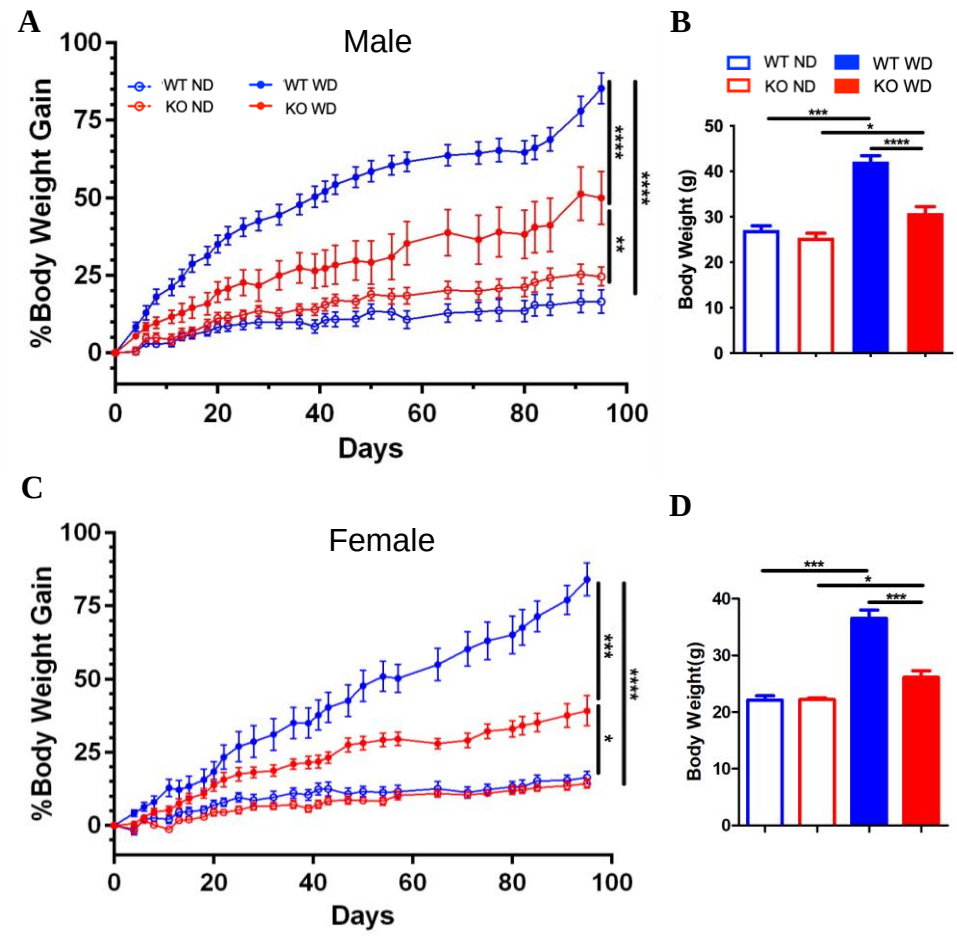

Figure 1. Male and female body weight change, final body weight, and representative photographs

(A) Male %body weight change, (B) male final body weight, (C) female %body weight change, (D) female final body weight of each group normal diet (ND), western diet (WD), wildtype (WT), and knockout (KO) are presented (n=20-30/group). All data are presented as mean ± SEM. One-way ANOVA with Tukey's test for post analysis was done. *P<0.05 **P<0.01, ***P<0.005, ****P<0.001

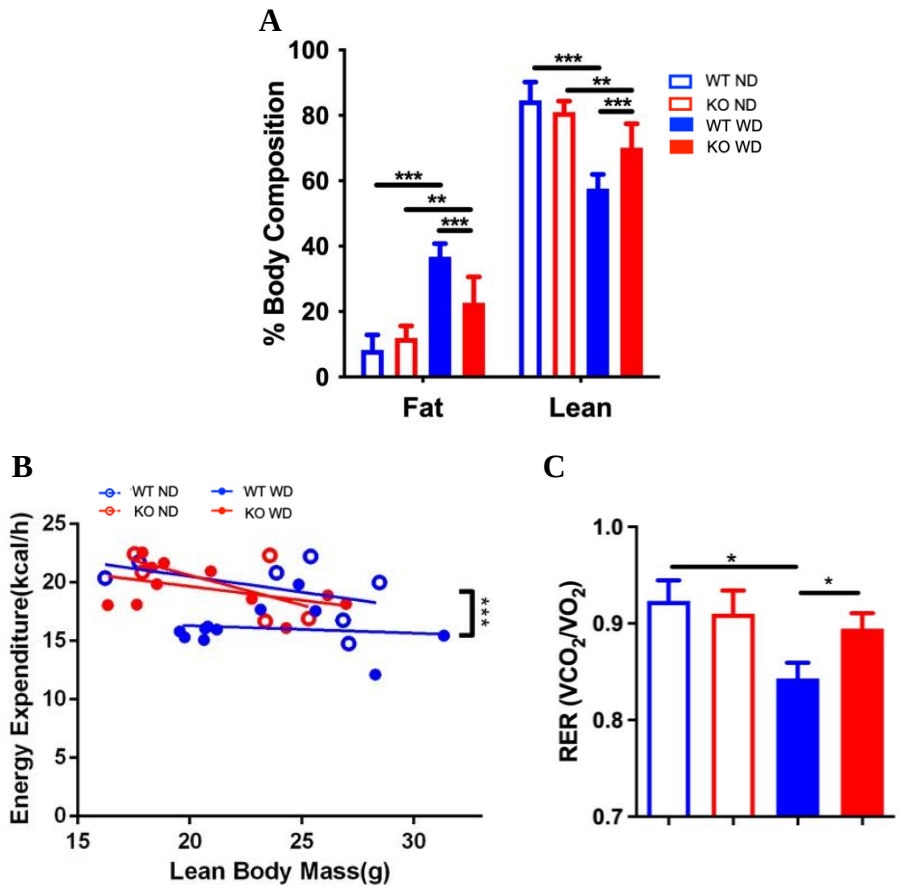

Figure 2. Body composition, energy expenditure by lean body mass, and respiratory exchange ratio

(A) % Body composition, (B) energy expenditure, and (C) respiratory exchange ratio (RER) were measured during 2 days in CLAMS metabolic cage of each group (n=5-11/group). Analysis of covariance (ANCOVA) was used for analyzing energy expenditure with lean body mass as covariate. RER was calculated by VCO_2/VO_2. All data are presented as mean ± SEM. One-way ANOVA with Tukey's test for post analysis was done. *P<0.05, **P<0.01, ***P<0.005

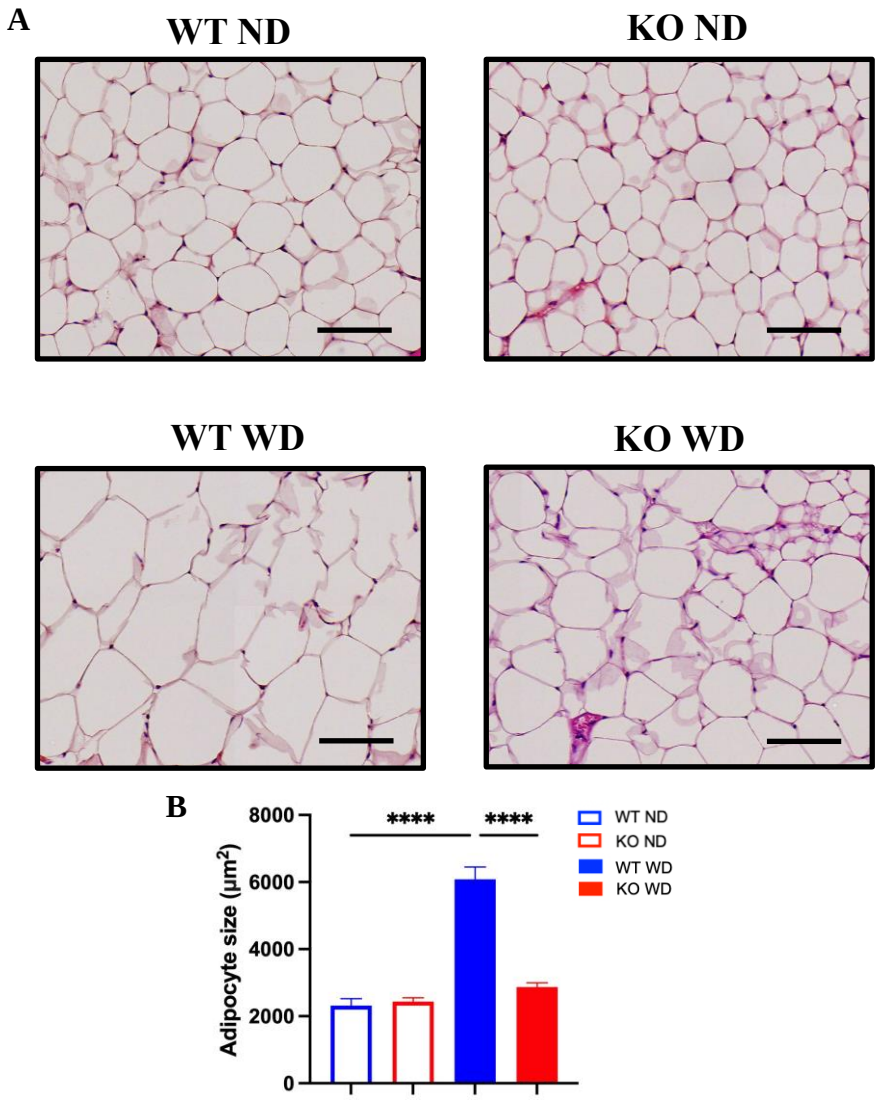

Figure 3. Histological analysis of white adipose tissue

(A) Microscopically scanned hematoxylin and eosin (H&E) staining of abdominal white adipose tissues (WAT) and (B) measured average adipocyte size (μm^2) of each WT ND, KO ND, WT WD, KO WD are presented (n=4/group). All data are presented as mean ± SEM. Microscopic scans are displayed at 50× magnification. Scale bar size=100μm. One-way ANOVA with Tukey's test for post analysis was done.

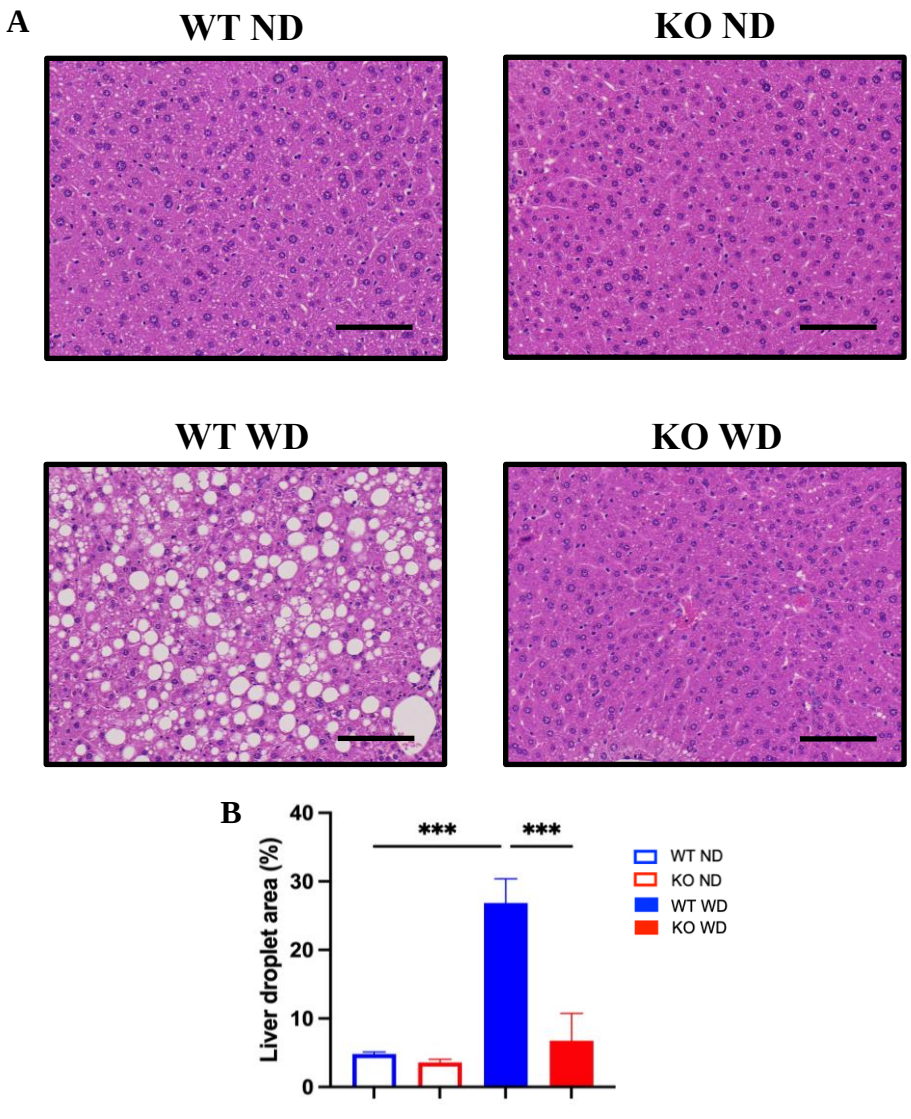

Figure 4. Histological analysis of liver tissues

(A) Microscopically scanned hematoxylin and eosin (H&E) staining of liver tissues and (B) measured liver droplet area (%) of each WT ND, KO ND, WT WD, KO WD are presented (n=4/group). All data are presented as mean ± SEM. Microscopic scans are displayed at 50× magnification. Scale bar size=100μm. One-way ANOVA with Tukey's test for post analysis was done. ***P<0.005

2. Difference in obesity development is not due to differential energy intake or activity rate

To investigate the cause of differential obesity development of western diet fed *Tas1r3*$^{+/+}$ and *Tas1r3*$^{-/-}$ mice, food intake was closely monitored during 14 weeks of diet induction. Since the Tas1r3 gene is related to taste sensing, it was possible that eliminating the gene would affect diet or liquid intake. Interestingly, despite the deficient sweet taste sensor in the tongue, *Tas1r3*$^{-/-}$ mice ate similar amount of western diet. The data showed that there were no differences in diet or water intake, thus no difference in caloric intake, between different genotypes. Only differences observed was between two diet groups (WT ND vs WT WD: $P<0.005$; KO ND vs KO WD: $P<0.005$) (**Figure 5**).

To understand the disparity in obesity development, individual activity rate was also recorded during 2 days of CLAMS metabolic assessment. As mice are nocturnal animals, during the light cycle of the day (0700-1900), activity counts were low. The western diet fed groups were more active during the light cycle ($P<0.01$). During the night cycle (1900-0700), there were no significant differences between experimental groups, but western diet fed groups showed tendency to be more active (**Figure 6**).

These results indicate that, even though same amount of nutrients entered and same amount of energy was consumed among the same diet group, *Tas1r3*$^{-/-}$ mice had little increase in body weight, less fat stored, and even normal unaffected liver. So, what happened to all the excess nutrients of *Tas1r3*$^{-/-}$ mice?

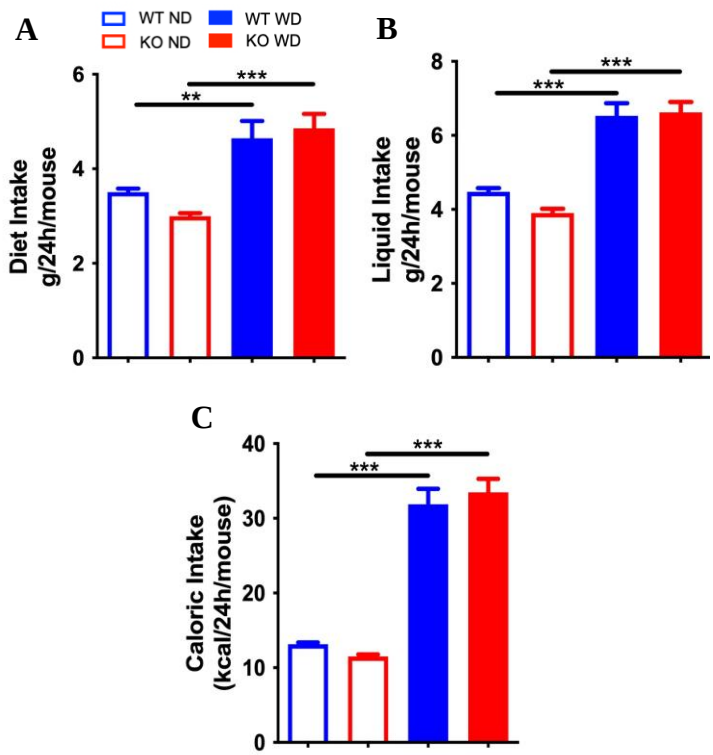

Figure 5. Diet, drink, and caloric intake

(A) Diet and (B) liquid intake were measured two times a week during diet induction period (n=20-30/group). (C) Caloric intake was calculated according to diet calories information provided in Table 2. and sucrose calories (4kcal/g). All data are presented as mean ± SEM. One-way ANOVA with Tukey's test for post analysis was done. *P<0.05, **P<0.01, ***P<0.005

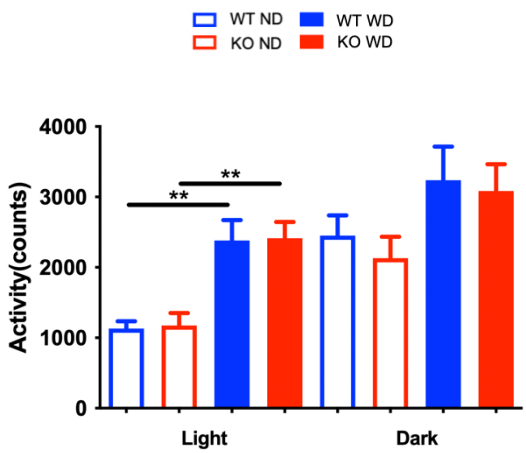

Figure 6. Activity counts during light and dark cycle

Activity counts were measured in CLAMS metabolic cages. Automated 12/12 light (0700-1900) and dark (1900-0700) cycles were implemented (n=5-11/group). All data are presented as mean ± SEM. One-way ANOVA with Tukey's test for post analysis was done. **P<0.01

3. Tas1r3 regulates intestinal transcriptional networks

Previous results showed that the normal diet groups do not have any differences in obesity development and energy intake. Western diet fed groups which showed the most significant differences were focused. Since the supposedly absorbed excess nutrients in *Tas1r3*$^{-/-}$ mice were nowhere to be found inside the body, the small intestine, that has high expression of TAS1R3, was the next suspect. To investigate how the missing taste sensing gene could affect other mechanisms in the small intestine, the transcriptomes of the small intestine were examined.

The principal component analysis showed that the gene profile of WD fed *Tas1r3*$^{-/-}$ mice were significantly different from *Tas1r3*$^{+/+}$ mice. The principal component 1 explained the differences between the two genotypes at 48.88% and the gene profile was exceedingly similar inside each group. The principal component 2 indicated that within a group of genotype male and female showed slight variance (**Figure 7**).

The volcano plot of differently expressed genes revealed that with adjusted P-values and fold changes for each and every single gene, which was calculated by different gene expression of WD fed *Tas1r3*$^{-/-}$ mice from *Tas1r3*$^{+/+}$ mice of same diet, there are an abundance of genes that are up or down regulated just with the absence of the *Tas1r3* gene (**Figure 8**).

As can be seen with the PCA plot, the hierarchical clustering computing of differentially expressed genes further showed that the two different genotype groups have distinct gene expression patterns. The clustering elucidates that the down or upregulated gene pool of *Tas1r3*$^{-/-}$ mice compared to *Tas1r3*$^{+/+}$ mice are the main two big clustering factors in the algorithm (**Figure 9**).

The gene interaction network created by the Ingenuity Pathway Analysis (IPA) shed light to which genes and signaling pathways are affected by the absence of *Tas1r3* gene (**Figure 11**).

By observing which group of genes were differently expressed in small intestine of *Tas1r3*$^{-/-}$ mice, it was found that the molecular transport and lipid metabolism related biological functions were significantly changed (**Figure 10**). Interestingly, CD36, which absorbs lipids in enterocytes, had reduced expression. Since TAS1R3 is expressed in enteroendocrine cells (EECs), not in nutrient absorbing enterocytes, EEC secreting hormone related genes were looked into. Glucagon-like peptide 2 receptors (GLP2R) and its downstream genes that contributes to lipid absorption (mTOR, SREBP) also had the same expression pattern (**Figure 12)**.

With the transcriptome analysis of WD fed *Tas1r3*$^{+/+}$ and *Tas1r3*$^{-/-}$ mice, lipid absorption related genes were down regulated in *Tas1r3*$^{-/-}$ mice. It is suspected that with absence of TAS1R3 gene in EECs, the GLP-2 hormone se-

cretion is inhibited. The reduced GLP-2 secretion then affects the neighboring enterocytes, that are supposed to receive signals to absorb the abundant lipids by GLP-2 hormone, to not absorb the lipids by downstream signals (**Figure 12**).

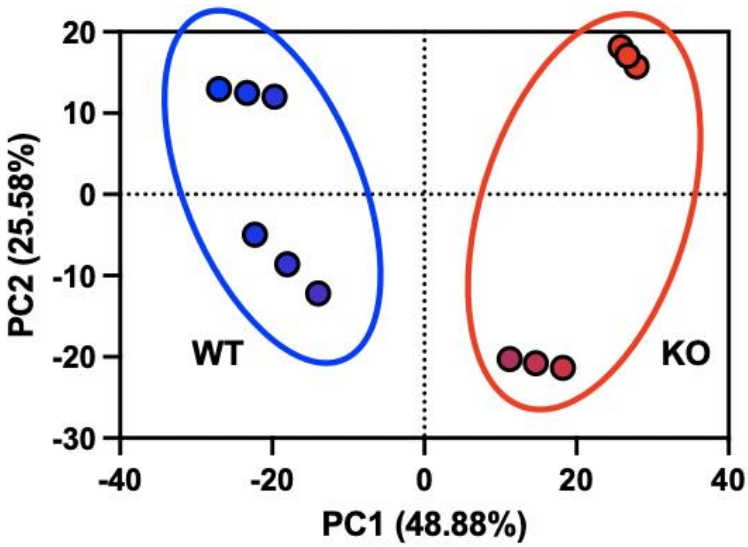

Figure 7. Principal component analysis of small intestine transcriptome

Principal component analysis (PCA) plot of small intestine transcriptome presented 2-dimensionally with principal component 1 (PC1) (48.88%) as X axis and PC2 (25.58%) as Y axis. Each point represents an individual mouse (n=6/group). Blue represents WT WD red represents KO WD.

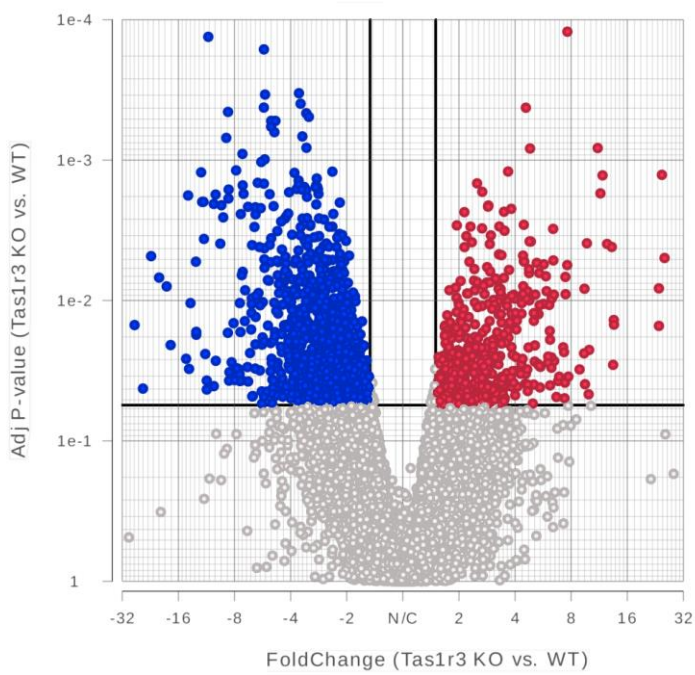

Figure 8. Volcano plot of differentially expressed genes

Volcano plot of differentially expressed genes (DEGs). Fold change was calculated by the ratio of KO WD and WT WD (n=6/group). P-values were adjusted with false discovery rate (FDR). Each point represents a single gene. Blue represents down regulated genes; red represents up regulated genes.

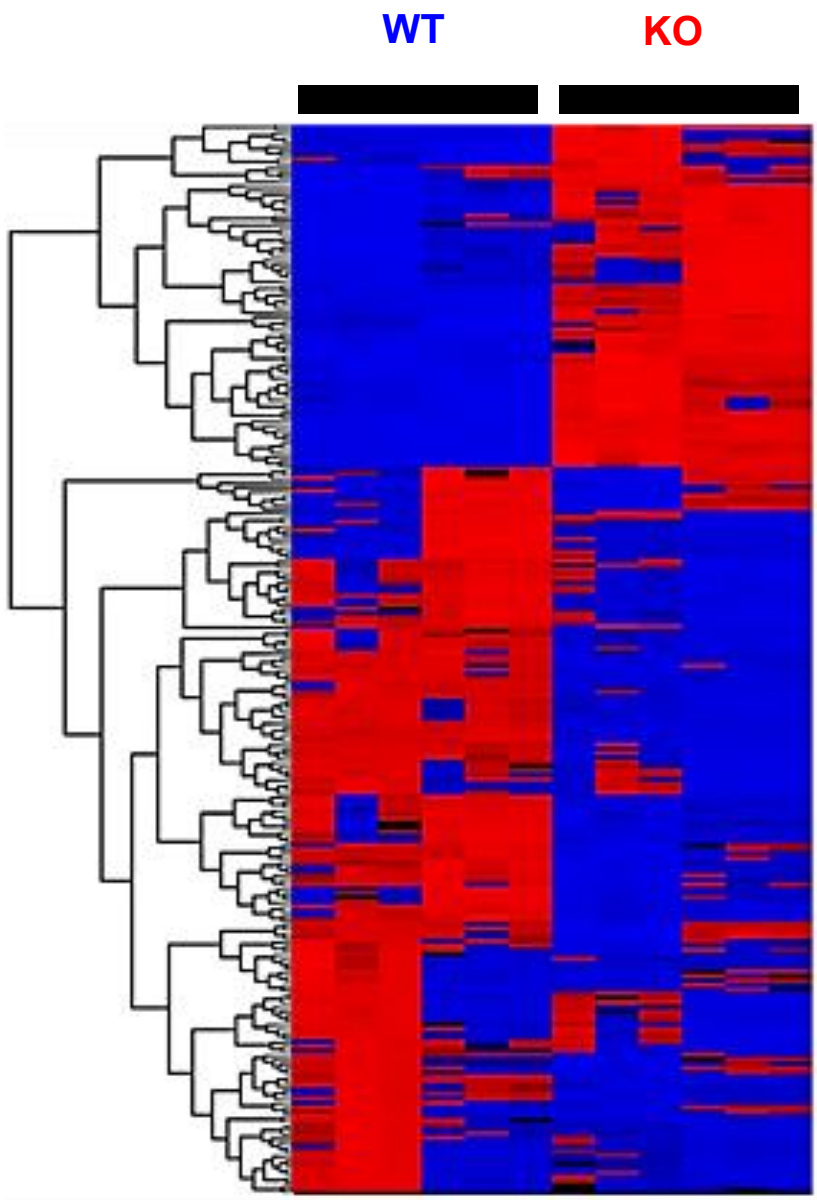
WT
KO

Figure 9. Hierarchical clustering of differentially expressed genes

Hierarchical clustering of differentially expressed genes that were up or down regulated. Only WD fed mice WT (*Tas1r3*$^{+/+}$) and KO (*Tas1r3*$^{-/-}$) were included (n=6/group). WT WD vs KO WD was hierarchically clustered with the use of complete linkage method and the Euclidean distance metric. Red color indicates the up regulated genes and the blue color indicates the down regulated genes.

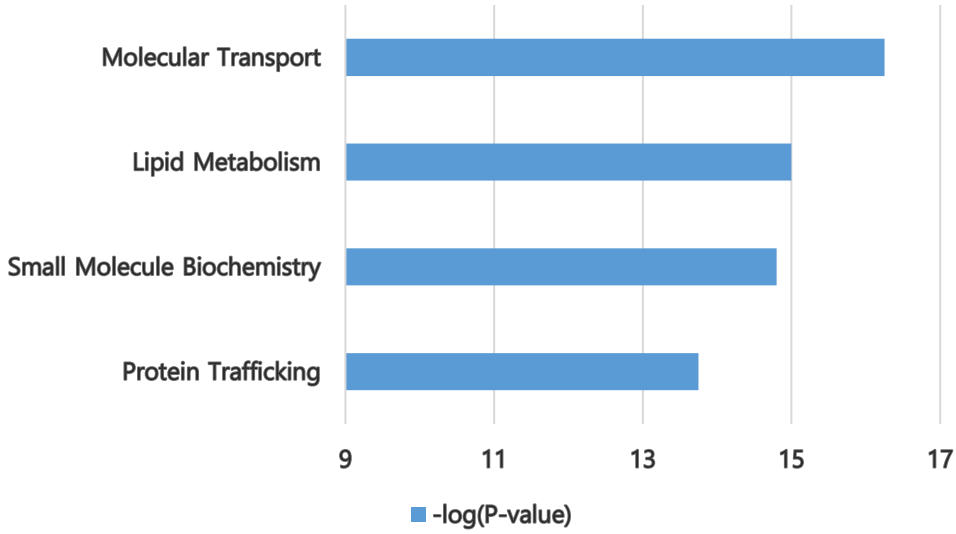

Figure 10. Functional classification of differentially expressed genes. Functional classification of differentially expressed genes computed by IPA (n=6/group). The representative figure shows significantly changed functions in WD fed *Tas1r3*$^{-/-}$ mice intestine compared to *Tas1r3*$^{+/+}$ mice. The biological functions are presented with -log(P-value).

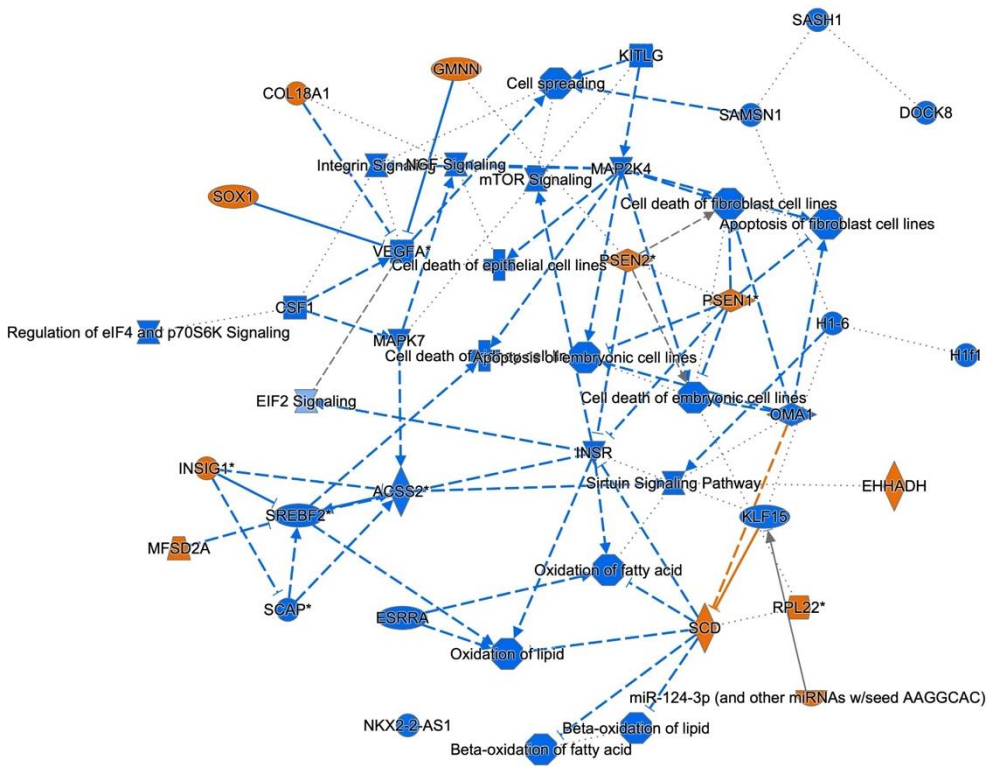

Figure 11. Gene interaction network

Gene interaction network of differentially expressed genes created by the IPA (n=6/group). Cutoff P-value was 0.001. Blue filled nodes are down regulated, and orange filled nodes are up regulated. DEGs of WT WD vs. KO WD were used in the analysis.

A

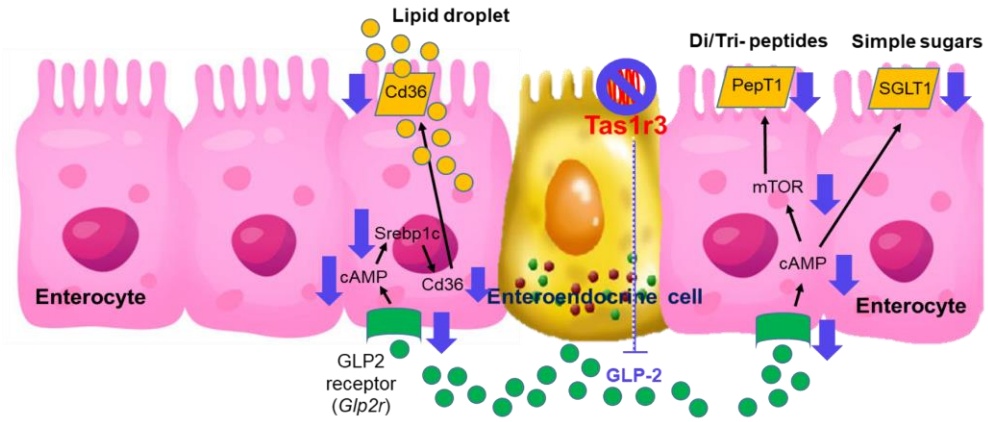
Lipid droplet
Cd36
Tas1r3
Di/Tri- peptides
Simple sugars
PepT1
SGLT1
mTOR
Srebp1c
cAMP
Cd36
cAMP
Enterocyte
Enteroendocrine cell
Enterocyte
GLP2
receptor
(Glp2r)
GLP-2

B

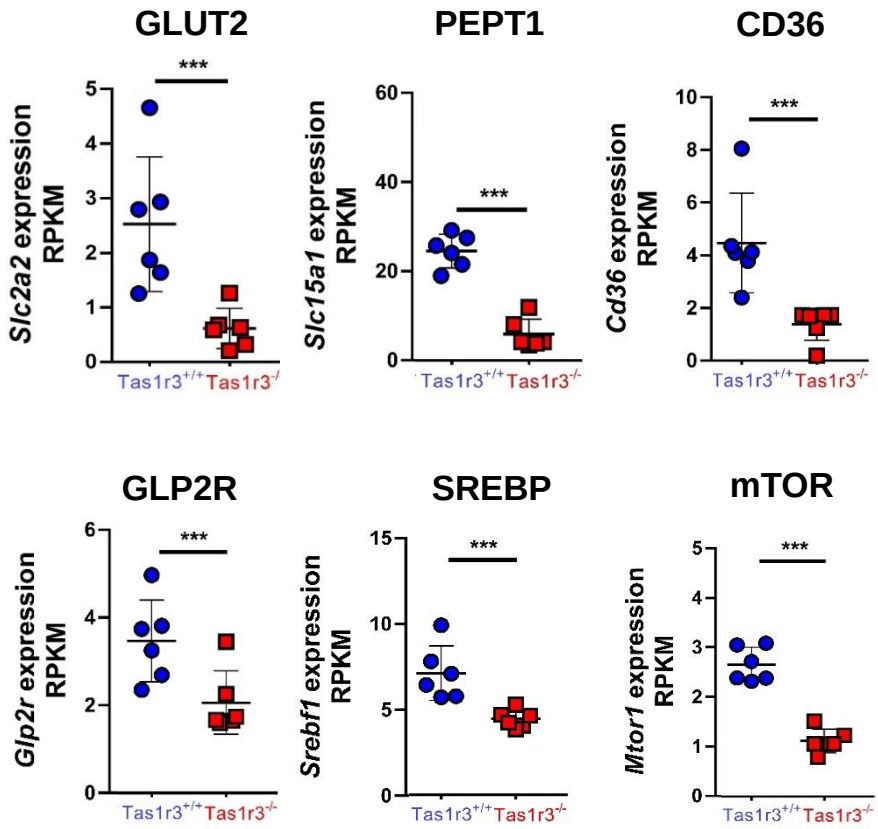
GLUT2
PEPT1
CD36
Slc2a2 expression RPKM
Slc15a1 expression RPKM
Cd36 expression RPKM
***
Tas1r3+/+ Tas1r3-/-
GLP2R
SREBP
mTOR
Glp2r expression RPKM
Srebf1 expression RPKM
Mtor1 expression RPKM

Figure 12. Predicted intestinal TAS1R3 signaling pathway

(A) Enteroendocrine cells (EECs) expressing TAS1R3 secretes glucagon-like peptide 2 (GLP-2) to activate the GLP-2 receptor and its downstream signaling to absorb lipids. (B) Glucose transporter 2 (GLUT2), peptide transporter 1 (PEPT1), cluster of differentiation 36 (CD36) expressions in the intestine of WT WD and KO WD. Glucagon-like peptide 2 receptor (GLP2R), sterol regulatory element-binding protein (SREBP), mammalian target of rapamycin (mTOR) expressions (n=6/group). Gene expression levels are shown in reads per kilobase of transcript, per million mapped reads (RPKM).

4. Tas1r3 deficiency attenuates lipid absorption in the small intestine

The transcriptome analysis revealed that fat absorption related genes had reduced expression. To confirm the results, lipid absorption in the intestine was measured. First, the residual lipid amount in the feces of each mouse was analyzed. Surprisingly the lipid amount in the feces of *Tas1r3*$^{-/-}$ mice were higher than the *Tas1r3*$^{+/+}$ mice ($P<0.05$). The ANCOVA analysis with body weight showed that the body weight difference between two groups did not account for the excreted lipids (correlation of WT vs. KO: P=0.5007 vs. P=0.5054). However, as fat intake as the covariate, *Tas1r3*$^{-/-}$ mice had positive correlation with the covariate while *Tas1r3*$^{+/+}$ mice did not (correlation of WT vs. KO: P=0.3002 vs. P=0.0364; **Figure 13**).

To further confirm the impaired lipid absorption, the residual lipid levels after feeding olive oil in the small intestine of the mice were measured. The TG level in the *Tas1r3*$^{-/-}$ mice were higher than the *Tas1r3*$^{+/+}$ mice ($P<0.05$). The TC level did not differ between two groups (P=0.9061, **Figure 14**).

Higher fecal lipid and higher TG levels in the small intestine of *Tas1r3*$^{-/-}$ mice confirm the transcriptome analysis that lipid absorption related gene expression is reduced. The obesity resistance *Tas1r3*$^{-/-}$ mice possess, is due to inhibited lipid absorption in the small intestine.

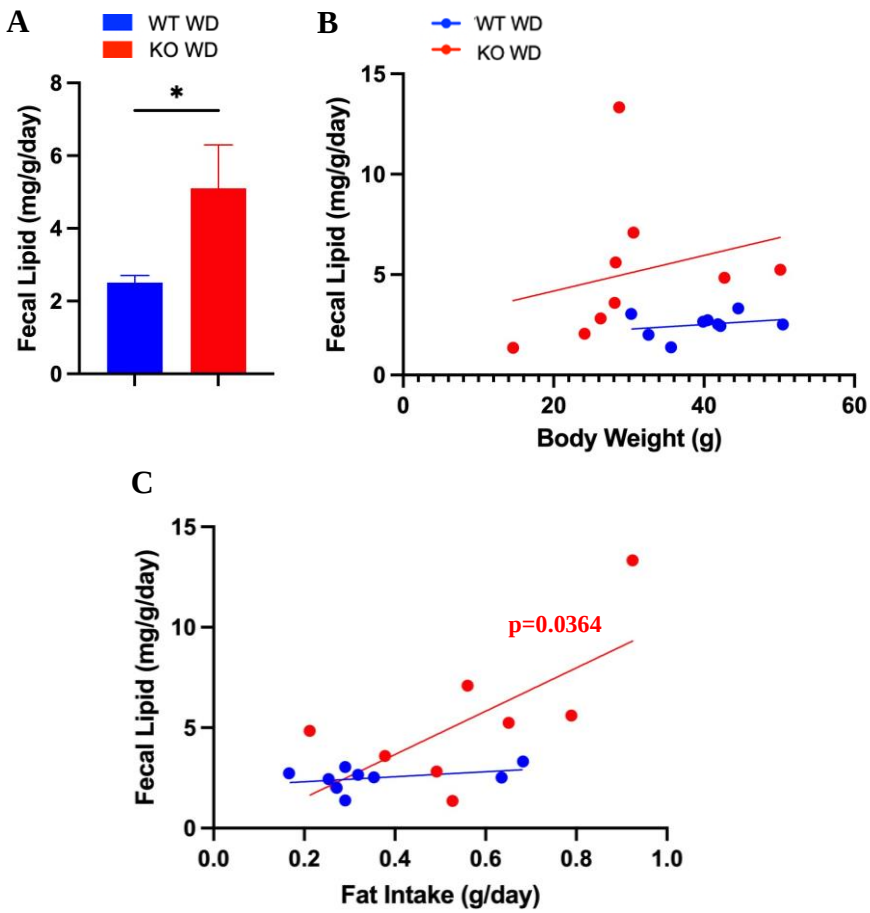

Figure 13. Fecal lipid analysis

(A) Leftover lipid amount in the feces of WT WD and KO WD group (n=9/group). The ANCOVA analysis of fecal lipid with (B) body weight and (C) fat intake as covariates. Fat intake was measured with diet intake and provided composition of the diets (**Table 2**). Student's T-test and simple linear regression analysis was done. *P<0.05

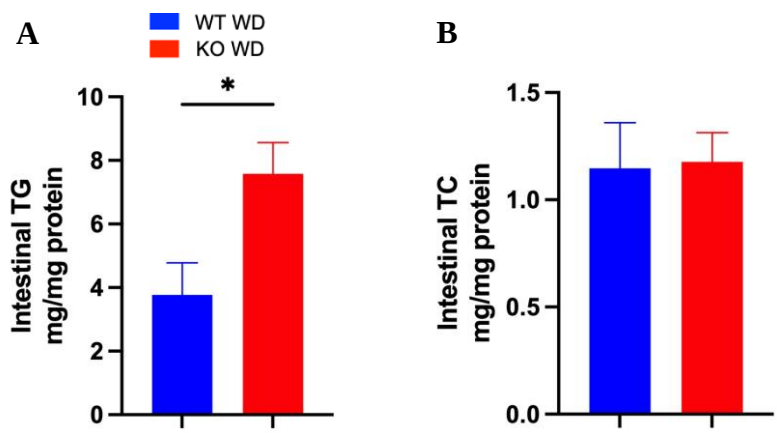

Figure 14. Intestinal triglyceride and total cholesterol level

(A) Residual TG and (B) TC levels in intestinal tissues of WT WD and KO WD groups after olive oil oral gavage (n=5/group). Oral gavage was administered (1.0 mg/g body weight) after 12 hours of fasting. Intestinal tissues were collected after 4 hours. Tissue protein level was used for correction. Student's T-test was done for analysis. *P<0.05

IV. Discussion

TAS1R3 function in the body is prominently linked to sensing taste in the tongue. TAS1R3 senses amino acids with the help of TAS1R1, and fructose with the help of TAS1R2 (Zhao et al., 2003). The taste sensing protein is also expressed in extra-oral tissues, such as intestine and brain, and is suspected to have other functions than sensing taste (Depoortere, 2014). However, the exact role of TAS1R3 in the intestine has not yet been published. In this study the role of intestinal TAS1R3 in development of obesity and its possible signaling network were examined.

To identify the roles of TAS1R3 in diet-induced obesity, the knockout of the gene and diet-induced obesity model were employed. Specifically, western diet composed of high fat diet with high sucrose drink was selected, as western diet is associated with obesity (Eng et al., 2020). Normal diet eating mice, whether it be *Tas1r3*$^{+/+}$ mice or *Tas1r3*$^{-/-}$ mice, showed no difference in body weight or other obesity parameters. However, 14 weeks of high fat diet and sugar drink had impact on the *Tas1r3*$^{+/+}$ mice. They had gained weight by approximately 75%, increased fat percentage, and decreased respiratory exchange ratio and energy expenditure, which are all symptoms of obesity (Blüher, 2019). Distinctively, the WD fed *Tas1r3*$^{-/-}$ mice showed little or no symptoms of obesity. Slightly increased body weight and body fat

was observed, but respiratory exchange ratio and energy expenditure were not different from normal diet fed counterpart. These results left a question about what causes this disparity between the two genotypes.

The lack of taste receptors in the tongue or the intestine could have altered the eating patterns of *Tas1r3*$^{-/-}$ mice. The record of diet and drink intake patterns were not different between two groups. TAS1R3 did not affect diet and drink intake, thus the obesity did not derive from energy intake. This result matches the results of other previous studies (Damak et al., 2003; Sclafani et al., 2010; Glendinning et al., 2012). TAS1R3 knockout mice has been reported to have altered social behavior and learning, but in simple activity counts there were no differences derived from deprivation of the gene (Martin et al., 2017). The only difference observed in activity count was during the light cycle where western diet fed groups were more active. During the dark cycle western diet fed groups showed more activity but there was no significance. This elevated activity rate in western diet groups could be explained by the correlation between western diet and anxiety (Jacka et al., 2010). In C57BL/6J mice anxiety has been associated with high locomotor activity (Carola et al., 2010) Obesity resistance in *Tas1r3*$^{-/-}$ mice was not due to decreased nutrient intake or hyperactivity. These findings led to the assumption that TAS1R3 played an important intrinsic role in obesity development in *Tas1r3*$^{+/+}$ mice.

The histology of adipose tissues confirmed that fat accumulation occurred in TAS1R3 wildtype mice with high fat, high sugar while TAS1R3 knockout mice did not. The histology of liver tissues also revealed that WD fed wildtype mice developed fatty liver. All of these observation advocates the theory that TAS1R3 plays an important part in development of obesity.

The identical intake pattern of the two different genotypes showed same excess amount of nutrients and energy was introduced into the system. However, only one genotype had developed obesity. The oversupply of nutrients was nowhere to be found in the knockout mice. If the absorbed nutrients were not in the body, it meant the nutrients were not absorbed in the first place (Zhang et al., 2018; Kim et al., 2020).

TAS1R3 is known to be expressed in the gut and the exact role is yet to be uncovered (Depoortere, 2014). Multiple experiments reported that TAS1R3 regulates mTORC1 on various tissues which is known to control lipid metabolism (Wauson et al., 2012; Shojaat et al., 2020; Laplante et al., 2009). Also, TAS1R3 has already been reported to regulate SGLT1 expression in the intestine (Margolskee et al., 2007).

The principal component analysis of WD groups showed that same genotype of mice had similar gene profiles. Principal component 2 had shown there were sex differences. This may be caused by the differential effect of sex hormones on various parts (Mosinger et al., 2013; Palmisano et al.,

2018), however there were no visible phenotype differences between male and female mice in our experiments. Further investigation is required for sex-related differences. Volcano plot summarized the existence of multiple differentially expressed genes that are down or up regulated in the knockout mice compared to wildtype mice. Hierarchical clustering of differentially express genes and gene interaction network shows comprehensive understating of effects of TAS1R3 on the transcriptional level.

Functional classification of differentially expressed genes revealed that molecular transport and lipid metabolism related functions changed dramatically in WD fed *Tas1r3*$^{-/-}$ mice. Notably, CD36, which is a transporter that absorbs lipids in enterocytes, were down regulated (Cifarelli et al., 2018). However, TAS1R3 is not expressed in enterocytes, but in enteroendocrine cells (EEC) (Kokrashvili et al., 2014). The TAS1R3 expressed EECs would have affected the neighboring enterocytes by paracrine signaling. Surprisingly, glucagon-like peptide 2 receptor (GLP2R) expression was also reduced. EEC secreted GLP-2 increases intestinal lipid absorption by upregulating CD36 (Hsieh et al., 2009). The reduced secretion of GLP-2 hormone affected the downregulation of GLP2R in enterocytes. GLP-2 receptors are G-proteins coupled receptors that affects cAMP signaling pathways (Dubé & Brubaker, 2007). The down regulated cAMP signaling pathway regulates the expression of sterol regulatory element binding protein (SREBP) and mammalian

target of rapamycin (mTOR) which is crucial for lipid absorption and metabolism (Halder et al., 2002; Wauson et al., 2012; Shojaat et al, 2020; Laplante et al., 2009). The repressed activity of SREBP and mTOR with the absence of TAS1R3 could have decreased lipid absorption in the intestine by inactivation of CD36 (Ko et al., 2020). With all of these genes down regulated, lipid absorption could be impaired in the knockout mice.

To confirm the effect of down regulated lipid absorption related genes, intestinal lipid absorption rate was measured. The fecal lipid amount in WD fed groups was significantly different. Knockout mice excreted more lipids in the feces. ANCOVA with body weight as covariate showed body weight did not affect lipid secretion in feces. However, with fat intake as covariate, knockout mice showed increased secretion as fat intake increased. Positive correlation between fecal lipid amount and fat intake was observed. Combining the high level of residual TG in the small intestine, these analyses confirmed the results of transcriptome analysis that TAS1R3 knockout mice have impaired lipid absorption in the intestine.

Collectively, this study demonstrates that TAS1R3 is an important part of obesity development. Without TAS1R3, the knockout mice had not developed obesity, with no metabolic disorders found. The transcriptome analysis of small intestine of mice shows probable theories of how TAS1R3 regulated

other genes to cause the outcome. The obesity resistance of TAS1R3 deficient mice seems to have originated from impaired fat absorption in the intestine. While prevalence of obesity rises, further investigation of the exact mechanism of TAS1R3 signaling network could provide a solution to preventing and treating obesity.

References

Bhaskaran K, Douglas I, Forbes H, dos-Santos-Silva I, Leon DA, Smeeth L. **Body-mass index and risk of 22 specific cancers: a population-based cohort study of 5·24 million UK adults.** *Lancet.* 2014;384(9945):755-65.

Blüher M. **Obesity: global epidemiology and pathogenesis.** *Nature Reviews Endocrinology*. 2019;15(5):288-298.

Cameron AJ, Shaw JE, Zimmet PZ. **The metabolic syndrome: prevalence in worldwide populations**. *Endocrinology and Metabolism Clinics of North America.* 2004;33(2):351-75, table of contents.

Carola V, D'Olimpio F, Brunamonti E, Mangia F, Renzi P. **Evaluation of the elevated plus-maze and open-field tests for the assessment of anxiety-related behaviour in inbred mice**. *Behavioural Brain Research.* 2002;134(1-2):49-57.

Cifarelli V, Abumrad NA. **Intestinal CD36 and Other Key Proteins of Lipid Utilization: Role in Absorption and Gut Homeostasis**. *Comprehensive Physiology*. 2018;8(2):493-507.

Conway B, Rene A. **Obesity as a disease: no lightweight matter.** *Obesity Reviews.* 2004;5(3):145-51.

Damak S, Rong M, Yasumatsu K, Kokrashvili Z, Varadarajan V, Zou S, Jiang P, Ninomiya Y, Margolskee RF. **Detection of sweet and umami taste in the absence of taste receptor T1r3.** *Science.* 2003;301(5634):850-3.

Depoortere I. **Taste receptors of the gut: emerging roles in health and disease.** *Gut*. 2014;63(1):179-90.

Dubé PE, Brubaker PL. **Frontiers in glucagon-like peptide-2: multiple actions, multiple mediators.** *American Journal of Physiology Endocrinology and Metabolism*. 2007;293(2):E460-5.

Eng JY, Moy FM, Bulgiba A, Rampal S. **Dose-Response Relationship between Western Diet and Being Overweight among Teachers in Malaysia.** *Nutrients.* 2020;12(10):3092.

Filippatos TD, Derdemezis CS, Gazi IF, Nakou ES, Mikhailidis DP, Elisaf MS. **Orlistat-associated adverse effects and drug interactions: a critical review.** *Drug Safety*. 2008;31(1):53-65.

Folch J, Lees M, Sloane Stanley GH. **A simple method for the isolation and purification of total lipides from animal tissues.** *Journal of Biological Chemistry*. 1957;226(1):497-509.

Glendinning JI, Gillman J, Zamer H, Margolskee RF, Sclafani A. **The role of T1r3 and Trpm5 in carbohydrate-induced obesity in mice.** *Physiology & Behavior*. 2012;107(1):50-8.

Halder SK, Fink M, Waterman MR, Rozman D. A. **cAMP-responsive element binding site is essential for sterol regulation of the human lanosterol 14alpha-demethylase gene (CYP51).** *Molecular Endocrinology*. 2002;16(8):1853-63.

Hales CM, Carroll MD, Fryar CD, Ogden CL. **Prevalence of Obesity and Severe Obesity Among Adults: United States, 2017-2018.** *NCHS Data Brief*. 2020;(360):1-8.

Hsieh J, Longuet C, Maida A, Bahrami J, Xu E, Baker CL, Brubaker PL, Drucker DJ, Adeli K. **Glucagon-like peptide-2 increases intestinal lipid absorption and chylomicron production via CD36.** *Gastroenterology*. 2009;137(3):997-1005, 1005.e1-4.

Hu FB, van Dam RM, Liu S. **Diet and risk of Type II diabetes: the role of types of fat and carbohydrate.** *Diabetologia*. 2001;44(7):805-17

Jacka FN, Pasco JA, Mykletun A, Williams LJ, Hodge AM, O'Reilly SL, Nicholson GC, Kotowicz MA, Berk M. **Association of Western and traditional diets with depression and anxiety in women**. *American Journal of Psychiatry*. 2010;167(3):305-11

Jackson VM, Breen DM, Fortin JP, Liou A, Kuzmiski JB, Loomis AK, Rives ML, Shah B, Carpino PA. **Latest approaches for the treatment of obesity.** *Expert Opinion on Drug Discovery*. 2015;10(8):825-39.

Khera R, Murad MH, Chandar AK, Dulai PS, Wang Z, Prokop LJ, Loomba R, Camilleri M, Singh S. **Association of Pharmacological Treatments for Obesity With Weight Loss and Adverse Events: A Systematic Review and Meta-analysis.** *JAMA.* 2016;315(22):2424-34.

Kim J, Kim H, Noh SH, Jang DG, Park SY, Min D, Kim H, Kweon HS, Kim H, Aum S, Seo S, Choi CS, Kim H, Kim JW, Moon SJ, Gee HY, Lee MG. **Grasp55$^{-/-}$ mice display impaired fat absorption and resistance to high-fat diet-induced obesity.** *Nature Communication.* 2020;11(1):1418.

Ko CW, Qu J, Black DD, Tso P. **Regulation of intestinal lipid metabolism: current concepts and relevance to disease.** *Nature Reviews Gastroenterology & Hepatology*. 2020;17(3):169-183.

Kokrashvili Z, Yee KK, Ilegems E, Iwatsuki K, Li Y, Mosinger B, Margolskee RF. **Endocrine taste cells.** *British Journal of Nutrition*. 2014;111 Suppl 1(01):S23-9.

Kopelman PG. **Obesity as a medical problem.** *Nature.* 2000;404(6778):635-43.

Kopp W. How Western Diet And Lifestyle Drive **The Pandemic Of Obesity And Civilization Diseases.** *Diabetes, Metabolic Syndrrome and Obesity.* 2019;12:2221-2236.

Laplante M, Sabatini DM. **An emerging role of mTOR in lipid biosynthesis.** *Current Biology.* 2009;19(22):R1046-52.

Lee JY. **Differential Hepatic Transcriptional Networks Regulated by High Sugar Consumption in Normal and High Fat-fed Mice.** [Unpublished master's thesis]. Seoul National University. 2015

Lee PL, Jung SM, Guertin DA. **The Complex Roles of Mechanistic Target of Rapamycin in Adipocytes and Beyond.** *Trends in Endocrinology & Metabolism.* 2017;28(5):319-339.

Luppino FS, de Wit LM, Bouvy PF, Stijnen T, Cuijpers P, Penninx BW, Zitman FG. **Overweight, obesity, and depression: a systematic review and meta-analysis of longitudinal studies.** *Archives of General Psychiatry*. 2010;67(3):220-9.

Margolskee RF, Dyer J, Kokrashvili Z, Salmon KS, Ilegems E, Daly K, Maillet EL, Ninomiya Y, Mosinger B, Shirazi-Beechey SP**. T1R3 and gustducin in gut sense sugars to regulate expression of Na^+-glucose co-transporter 1.** *Proceeding of National Academy of Sciences of the United States of America.* 2007;104(38):15075-80.

Martin B, Wang R, Cong WN, Daimon CM, Wu WW, Ni B, Becker KG, Lehrmann E, Wood WH 3rd, Zhang Y, Etienne H, van Gastel J, Azmi A, Janssens J, Maudsley S. **Altered learning, memory, and social behavior in type 1 taste receptor subunit 3 knock-out mice are associated with neuronal dysfunction.** *Journal of Biological Chemistry.* 2017;292(27):11508-11530.

Merigo F, Benati D, Cristofoletti M, Amarù F, Osculati F, Sbarbati A. **Glucose transporter/T1R3-expressing cells in rat tracheal epithelium.** *Journal of Anatomty*. 2012;221(2):138-50.

Mosinger B, Redding KM, Parker MR, Yevshayeva V, Yee KK, Dyomina K, Li Y, Margolskee RF. **Genetic loss or pharmacological blockade of testes-expressed taste genes causes male sterility.** *Proceeding of National Academy of Sciences of the United States of America.* 2013;110(30):12319-24.

Murovets VO, Bachmanov AA, Travnikov SV, Churikova AA, Zolotarev VA. **The Involvement of the T1R3 Receptor Protein in the Control of**

Glucose Metabolism in Mice at Different Levels of Glycemia. *Journal of Evolutional Biochemistry and Physiology.* 2014;50(4):334-344.

Murovets VO, Bachmanov AA, Zolotarev VA. **Impaired Glucose Metabolism in Mice Lacking the Tas1r3 Taste Receptor Gene**. *PLoS One.* 2015;10(6):e0130997

Murovets VO, Sozontov EA, Zachepilo TG. **The Effect of the Taste Receptor Protein T1R3 on the Development of Islet Tissue of the Murine Pancreas.** *Doklady Biological Sciences.* 2019;484(1):1-4.

Palmisano BT, Zhu L, Eckel RH, Stafford JM. **Sex differences in lipid and lipoprotein metabolism.** *Molecular Metabolism*. 2018;15:45-55.

Park MY. **Effects of High Sugar Consumption on Transcriptome of Adipose Tissues and Metabolome of Blood in Mice,** [Unpublished master's thesis]. Seoul National University. 2017

Parlee SD, Lentz SI, Mori H, MacDougald OA. **Quantifying size and number of adipocytes in adipose tissue.** *Methods in Enzymology*. 2014;537:93-122.

Renaud HJ, Cui JY, Lu H, Klaassen CD. **Effect of diet on expression of genes involved in lipid metabolism, oxidative stress, and inflammation in mouse liver-insights into mechanisms of hepatic steatosis.** *PLoS One.* 2014;9(2):e88584.

Sclafani A, Glass DS, Margolskee RF, Glendinning JI. **Gut T1R3 sweet taste receptors do not mediate sucrose-conditioned flavor preferences in mice.** *American Journal of Physiology-Regulatory, Integrative and Comparative Physiology*. 2010;299(6):R1643-50.

Shojaat SS, Engman S, Hofferber J, Keomanivong F, Wauson EM. **Loss of the nutrient receptor Tas1R3 reduces atherosclerotic plaque accumulation and hepatic steatosis in ApoE$^{-/-}$ mice.** *Journal of Physiology and Biochemistry.* 2020;76(4):623-636.

Shon WJ. **Roles of Taste Receptor TAS1R3 in the Pathogenesis of Diet-Induced Colitis**. [Unpublished doctoral dissertation]. Seoul National University. 2020

Tremmel M, Gerdtham UG, Nilsson PM, Saha S. **Economic Burden of Obesity: A Systematic Literature Review.** *International Journal of Environmental Research and Public Health*. 2017;14(4):435.

Tschöp MH, Speakman JR, Arch JR, Auwerx J, Brüning JC, Chan L, Eckel RH, Farese RV Jr, Galgani JE, Hambly C, Herman MA, Horvath TL, Kahn BB, Kozma SC, Maratos-Flier E, Müller TD, Münzberg H, Pfluger PT, Plum L, Reitman ML, Rahmouni K, Shulman GI, Thomas G, Kahn CR, Ravussin E**. A guide to analysis of mouse energy metabolism.** *Nature Methods*. 2011;9(1):57-63.

Udagawa H, Hiramoto M, Kawaguchi M, Uebanso T, Ohara-Imaizumi M, Nammo T, Nishimura W, Yasuda K. **Characterization of the taste receptor-related G-protein, α-gustducin, in pancreatic β-cells.** *Journal of Diabetes Investigation.* 2020 Jul;11(4):814-822.

Wang F, Song X, Zhou L, Liang G, Huang F, Jiang G, Zhang L. **The down-regulation of sweet taste receptor signaling in enteroendocrine L-cells mediates 3-deoxyglucosone-induced attenuation of high glucose-stimulated GLP-1 secretion.** Archives of Physiology and Biochemistry. 2018;124(5):430-435.

Wauson EM, Zaganjor E, Lee AY, Guerra ML, Ghosh AB, Bookout AL, Chambers CP, Jivan A, McGlynn K, Hutchison MR, Deberardinis RJ, Cobb MH. **The G protein-coupled taste receptor T1R1/T1R3 regulates mTORC1 and autophagy**. *Molecular Cell*. 2012;47(6):851-62.

Xu H, Cupples LA, Stokes A, Liu CT. **Association of Obesity With Mortality Over 24 Years of Weight History: Findings From the Framingham Heart Study**. *JAMA Network Open.* 2018 Nov 2;1(7):e184587.

Zhang F, Zarkada G, Han J, Li J, Dubrac A, Ola R, Genet G, Boyé K, Michon P, Künzel SE, Camporez JP, Singh AK, Fong GH, Simons M, Tso P, Fernández-Hernando C, Shulman GI, Sessa WC, Eichmann A. **Lacteal junction zippering protects against diet-induced obesity.** *Science.* 2018;361(6402):599-603.

Zhao GQ, Zhang Y, Hoon MA, Chandrashekar J, Erlenbach I, Ryba NJ, Zuker CS. **The receptors for mammalian sweet and umami taste.** *Cell.* 2003;115(3):255-66.

국문초록

식이 유도 비만 발생과정에서의 Taste 1 Receptor 3의 역할 연구

서울대학교 대학원 식품영양학과
오 승 훈

세계적으로 유병율이 증가하고 있는 비만은 관상동맥 심장질환과 당뇨, 지방간을 비롯한 여러 대사 질환을 야기할 수 있으므로, 그 원인 규명과 예방이 매우 중요하다. 고지방식이와 고설탕음료를 특징으로 하는 서구식 식이는 비만 유발에 관여하는 주요한 환경적 요인 중 하나이다. 그러나, 서구식 식이가 비만을 어떻게 유발하는 지에 대한 분자생물학적 기전은 아직 완전히 규명되지 않았다. 미각수용체가 혀 뿐 만 아니라, 다양한 체 내 기관에서도 발현된다는 것이 최근 알려졌다. 그러나, 맛을 감지하는 기관이 아닌 기관에서의 미각 수용체 수행 역할은 거의 밝혀지지 않았다. TAS1R3 는 혀에서는 단맛과 감칠맛을 감지한다고 알려져 있으나,

다른 체내 기관에서의 비만과의 관련성은 연구된 바 없다. 본 연구에서는 미각수용체인 TAS1R3 이 비만 발달에 미치는 영향을 알아보고자 하였다. 이를 위하여, TAS1R3 유전자 결핍마우스를 이용하여 서구식 식이로 비만 유발과정의 생리학적, 분자생물학적 변화를 정상마우스인 Wild type 마우스와 비교하였다. 8-12 주령 사이의 *Tas1r3*$^{-/-}$ 마우스(KO)와 *Tas1r3*$^{+/+}$(WT)에게 각각 정상식이(ND) 또는 서구식 식이 (WD; 60% 고지방 식이 + 30% 설탕음료)를 14 주간 공급하였다 (n=20-30/group). 14 주간의 몸무게 변화를 측정한 결과, 정상 식이를 제공받은 WT 과 KO 사이에는 몸무게의 차이가 없었다. 예상한 바와 같이 WD 를 공급받은 WT 는 성공적으로 몸무게가 증가하였으나, WD 를 공급받은 KO 의 몸무게 증가량은 WT-WD 군에 비해 현저하게 적었다. 몸무게 증가량에 기인하는 체조직 구성성분을 분석해 본 결과, WT-WD 마우스는 체지방이 현저히 높았으며 (36.8%), 이에 비해 KO-WD 마우스는 유의적으로 체지방 비율이 낮았다 (22.7%). 또한 대사케이지에서의 대사율을 분석해 본 결과, WT-WD 마우스의 호흡교환율이 KO-WD 에 비해 현저히 낮았다. 흥미롭게도 WT-WD 와 KO-WD 사이에서는 칼로리 섭취량에는

차이가 없었으며, 또한 신체 활동량에도 차이를 보이지 않았다. KO 와 WT 사이의 비만도의 차이가 장에서의 에너지 흡수차이로 기인한 것인지 알아보기 위해, 장 조직의 전사체 분석을 실시하였다. PCA 와 hierarchical clustering 을 분석한 결과, 서구식 식이를 제공받은 WT 과 KO 마우스들은 유전자 발현체에 뚜렷한 차이가 있었다. 특히, KO-WD 마우스는 CD36, SREBP, mTOR 등 지방 흡수와 대사 관련된 유전자 발현이 현저히 낮은 것을 확인하였다. 소장 세포의 GLP-2 수용체 발현을 분석한 결과, TAS1R3 가 발현되지 않는 KO-WD 마우스에서는 현저히 낮게 발현되는 것을 확인 하였다 (2.7 RPKM vs. 3.6 RPKM). Gene interaction network 분석을 실시한 결과, KO-WD 마우스는 WT-WD 마우스에 비해 지방 흡수와 대사 관련된 mTOR, SREBP 등의 네트워크 활성이 저해된 것을 알 수 있었다. 실제 KO 마우스의 장에서의 지방 흡수가 저해됨을 알아보기 위해 변의 지질 농도를 분석한 결과, 서구식 식이를 먹은 KO 마우스는 WT 마우스에 비해 변에서 지질의 양이 매우 높았다. 이를 서구식 식이를 섭취한 양과의 관계를 분석한 결과, WT 마우스는 섭취한 지방량과 관계없이 일정한 지방을 변으로 내보내지만, KO 마우스는 지방을

많이 섭취할 수록 많이 배출하였다 (p=0.0364). 또한 올리브유를 oral gavage 한 후 소장에서 흡수를 측정한 결과, WT 마우스에 비해 KO 마우스의 소장 조직에서 지방이 혈액으로 이동 하지 않고 조직에 많이 남아 있었다. 본 실험은 서구식 식이로 유도되는 비만에서 TAS1R3 가 하는 역할에 대해 제시한 첫 연구이며, 이 연구를 통해 서구식 식이의 섭취가 소장에서 비만 발달에 영향을 끼치는 분자 생물학적 기전을 최초로 제시하였다. 본 연구 결과는, 서구식 식이와 소장 TAS1R3 의 새로운 관계를 바탕으로 비만의 예방과 치료의 새로운 방법을 제공할 것으로 예상된다.

주요어 : TAS1R3 (Taste 1 receptor member 3), 비만, 서구식 식이, 지방 흡수

학 번 : 2019 - 21991